Int J Clin Exp Pathol 2026;19(3):130-145
www.ijcep.com /ISSN:1936-2625/IJCEP0168790

Original Article

Prognostic value of fatty acid metabolism-related genes in colorectal cancer

Shuling Zhou[1,2*], Min Chen[2*], Zhikun Dong[3], Yong Yang[1], Xiaorui Shi[4], Huan Kang[5], Changbei Shi[4], Xuan Wang[3]

[1]Department of Radiology, Xi'an Hospital of Traditional Chinese Medicine, Xi'an 710016, Shaanxi, China; [2]Department of Oncology Radiotherapy, First Affiliated Hospital of Xi'an Jiaotong University, Xi'an 710061, Shaanxi, China; [3]Department of Pathology, First Affiliated Hospital of Xi'an Jiaotong University, Xi'an 710061, Shaanxi, China; [4]Department of Nuclear Medicine, Shaanxi Provincial Tumor Hospital, Xi'an 710061, Shaanxi, China; [5]Academy of Computer Science and Engineering, Xi'an University of Technology, Xi'an 710048, Shaanxi, China. [*]Equal contributors.

Received September 13, 2025; Accepted March 3, 2026; Epub March 15, 2026; Published March 30, 2026

Abstract: Purpose: Colon cancer (CC), a malignancy with high global incidence and mortality, remains a major public health burden. As a pivotal aspect of tumor metabolic reprogramming, fatty acid metabolism has drawn significant research interest. This study was designed to elucidate the relationship between fatty acid metabolism-related gene expression and prognosis in patients with CC. Method: We obtained the mRNA expression profiles and corresponding clinical information of colon cancers from The Cancer Genome Atlas (TCGA) database. Expression data of fatty acid metabolism-related genes and survival data were extracted for subsequent analysis. Univariate Cox regression and least absolute shrinkage and selection operator (LASSO) regression analyses were employed to identify fatty acid metabolism-related genes associated with prognosis in CC patients. Subsequently, a prognostic model based on these six genes was constructed to predict survival probability. Patients were stratified into high-risk and low-risk groups based on the model. Differences between the two groups were analyzed, including gene set enrichment analysis (GSEA), immune cell infiltration, immunotherapy efficacy, and immune checkpoint expression levels. Furthermore, a novel nomogram incorporating the risk score, age, gender, and clinical stage was developed to predict individual patient outcome. Finally, the expression levels of the identified risk genes were validated in cell lines using quantitative real-time PCR (qRT-PCR). Results: 449 CC and 41 normal samples were included in this study. A prognostic model based on six fatty acid metabolism-related genes (ENO3, ELOVL3, ACOT11, ALAD, ELOVL6, ACADL) were built to evaluate the prognosis of CC patients. Patients in the high-risk group had poorer overall survival than those in the low-risk group ($P < 0.001$), with AUC value of 0.701. M0 macrophage infiltration and T helper cells were higher in the high-risk group, and regulatory T cells (Tregs) and infiltration of natural killer cell (NK) cells was less. The expression levels of PD-1, LAG3, and CTLA4 were higher in high-risk patients, and the high-risk group had a higher TIDE score, indicating a worse response to immunotherapy. The Calibration plots, receiver operating characteristic (ROC) curve, and Decision Curve Analysis (DCA) all showed that the nomogram method can accurately predict the survival rate of CC patients. In addition, qRT-PCR showed downregulated expression of ACOT11, ALAD, and ACADL, and upregulated expression of ELOVL6 and ENO3 in all colon cancer cell lines tested. There was no significant difference in the expression level of ELOVL3 between colon cancer cells and colon epithelial lines. Conclusion: Targeting fatty acid metabolism-related genes represents a promising therapeutic strategy for colon cancer (CC) that could pave the way for personalized treatment and enhanced patient survival.

Keywords: Fatty acid metabolism, predictive model, colon cancer, immune

Introduction

Colon cancer (CC) is a significant gastrointestinal malignancy that threatens human life and health. It ranks third in the incidence of malignant tumors in the world, after lung cancer and breast cancer, and second in the death rate of malignant tumors, after lung cancer [1]. Notwithstanding the rapid advances in comprehensive oncologic treatments, the five-year survival rate for colon cancer (CC) patients remains suboptimal, not exceeding 65%. Moreover, patient

https://doi.org/10.62347/FCJB8964

prognosis is markedly heterogeneous across different disease stages [2, 3]. Hence, addressing this unmet clinical need requires the development of accurate prognostic tools to improve risk stratification and inform personalized therapeutic decisions for CC patients.

To fuel their rapid proliferation, tumor cells rewire their metabolism, a process driven by the heightened energy and biosynthetic demands of the growing tumor tissue [4]. Fatty acid metabolic reprogramming is characterized by enhanced uptake, *de novo* synthesis, and reduced oxidation of fatty acids in tumor tissues. This imbalance results in intracellular lipid accumulation, which ultimately drives tumor cell proliferation and metastasis [5-7]. Recently, therapeutically targeting fatty acid synthesis [8, 9] and oxidation [10-12] has emerged as a promising strategy in cancer treatment, offering a novel direction for comprehensive anti-tumor therapy.

Fatty acid metabolic reprogramming within the tumor microenvironment critically regulates immune cell function. For instance, in hepatocellular carcinoma, enhanced fatty acid oxidation promotes M2 polarization of tumor-associated macrophages. Conversely, inhibiting this metabolic pathway reverses the M2 phenotype and thereby suppresses tumor progression [13]. Synergy between fatty acid oxidation (FAO) enzymes and immune checkpoints promotes tumor growth. Specifically, enhanced FAO upregulates CD47 expression, facilitating immune escape and thereby driving the invasive progression of glioblastoma multiforme (GBM). Consequently, dual inhibition of FAO and immune checkpoints represents a potent therapeutic strategy [14]. Despite the potential role of fatty acid metabolism in tumor progression, a clear understanding of how related genes predict outcomes and guide immunotherapy is still lacking.

Our study identified six fatty acid metabolism-related genes (ENO3, ELOVL3, ACOT11, ALAD, ELOVL6, ACADL) significantly associated with survival outcome in colon cancer (CC) patients. Using these genes, we constructed a prognostic model for risk stratification. Patients were stratified into high- and low-risk groups based on this model, revealing significant intergroup differences in GSEA pathways, immune cell infiltration, predicted immunotherapy response, and immune checkpoint expression. Furthermore, we developed a novel nomogram that integrates this fatty acid metabolism-based risk signature with key clinical factors to improve prognostic prediction. In conclusion, targeting fatty acid metabolism-related genes represents a promising therapeutic strategy that may pave the way for personalized treatment and improved survival in CC.

Patients and methods

Data processing

The mRNA expression profile and corresponding clinical information of CC patients were downloaded from The Cancer Genome Atlas (TCGA) data portal (https://portal.gdc.cancer.gov/). Finally, 41 normal colon samples and 449 CC cases were included in this study. Additionally, the following clinical information was extracted for further analyses: gender, age, stage, T, N, M classification, survival status, and follow-up time. Data were extracted and arranged by R and Perl programming languages.

Inclusion criteria: The patient has been pathologically diagnosed with colon cancer.

Exclusion criteria: 1. The patient also has severe lipid metabolism disorders (e.g., familial hypercholesterolemia, severe fatty liver); 2. The patient also suffers from chronic diseases that affect fatty acid metabolism, such as diabetes mellitus, thyroid dysfunction and cardiovascular diseases; 3. The patient also has other tumors or has severe organ failure caused by tumor metastasis (hepatic, renal and cardiac insufficiency); 4. The patient has received radiotherapy, chemotherapy, targeted therapy or immunotherapy in the recent three months, which may interfere with metabolic indicators; 5. Patients with incomplete transcriptome data or survival data.

Obtain fatty acid metabolism-related genes

Fatty acid metabolism-related genes were derived from three authoritative sources: the Hallmark gene set, the KEGG pathway, and the Reactome database. These gene lists were merged and subsequently deduplicated to generate a consolidated, non-redundant gene set for analysis.

Table 1. Composition and volume of reagents for RNA reverse transcription system

Reverse Transcription Reagent Components	Volume
RNA template	≤ 1 μg total RNA
Primer Mix	1 μL
StarScript III All-in-one RT Mix	1 μL
5×StarScript III All-in-one RT Buffer	4 μL
Nuclease-free Water	Supplement to 20 μL

Fatty acid metabolism-related prognostic model in CC patients

In order to identify fatty acid metabolism-related genes associated with survival of CC patients, we further performed univariate and multivariate Cox regression analyses based on corresponding expression and survival data. Those genes associated with prognosis in the multivariate Cox regression analysis then proceeded to the least absolute shrinkage and selection operator (LASSO) Cox regression analysis. The independent prognostic fatty acid metabolism-related genes were selected to construct the prognostic model. The coefficients of these regulators were selected according to the optimal penalty parameter λ in the cross-validation method. The following formula was used to estimate the risk score of each CC patient: risk score = (coef1 × expression of gene 1) + (coef2 × expression of gene 2) + (coef3 × expression of gene 3) +...+ (coefn × expression of gene n), where "coef" refers to the coefficient, and expression of genes was the relative value of selected genes. The mean risk score was used as the cutoff value to separate patients into low- and high-risk groups.

ssGSEA and TIDE

To quantify immune cell infiltration levels in each tumor sample, we performed single-sample Gene Set Enrichment Analysis (ssGSEA) using the "GSVA" R package. Separately, the Tumor Immune Dysfunction and Exclusion (TIDE) algorithm (http://tide.dfci.harvard.edu/) was applied to calculate TIDE scores, which serves as a predictive metric for patient response to immunotherapy.

Establishment of nomogram system

A nomogram is a graphical tool that integrates multiple prognostic variables onto a single scale, allowing for the direct calculation of a total score and the estimation of an individual's risk probability. We constructed a nomogram incorporating the fatty acid metabolism-related risk score along with key clinical factors (age, gender, and AJCC stage). Its development involved two steps: first, univariate and multivariate Cox regression analyses identified independent prognostic factors in colon cancer (CC); second, these factors - age, gender, risk score, T status, N status, M status, and AJCC stage- were integrated into the final model. The predictive accuracy of the nomogram was assessed using calibration plots, which compare predicted versus observed survival probabilities, and by calculating the area under the receiver operating characteristic (ROC) curve (AUC).

Cell lines and culture

The NCM460 colorectal epithelial cell line and the SW480 and HCT116 colorectal cancer cell lines were obtained from the Culture Collection of the Chinese Academy of Sciences (Shanghai, China). NCM460 and HCT116 were cultured with DMEM high-sugar medium, while SW480 was cultured with RPMI 1640 medium. The medium contained 10% fetal bovine serum and 1% Penicillin-Streptomycin (100×) in a humid incubator containing 5% CO_2 and constant temperature at 37°C.

Real time quantitative PCR (RT-PCR)

Total cell RNA was extracted using RNAfast200 kit, RNA concentration was measured and recorded using NanoDrop 2000 instrument.

① RNA reverse transcription. Subsequently, RNA reverse transcription is performed. In a sterile and enzyme-free EP tube, add the required components sequentially in the following order in **Table 1**: Transfer the prepared mixture into a PCR machine for amplification reaction, with the specific reaction condition parameters set as follows in **Table 2**. After the reaction is completed, all the liquid in the EP tube is cDNA, which can be aliquoted and stored to avoid repeated freeze-thaw cycles. It should be placed in a -80°C freezer for future use.

② RT-qPCR detection. The reaction system is as follows in **Table 3**: After adding all the neces-

Table 2. Reaction conditions for RNA reverse transcription amplification

Reaction Temperature	Reaction Time
37°C	2 min
50°C	15 min
85°C	2 min

sary components of the qPCR reagents, transfer the resulting mixture into the PCR machine for subsequent detection and analysis, the results are shown in **Table 4**: The primer sequences were as follows: GAPDH Forward: GGAGTCCACTGGCGTCTTCA, Reverse: GTCATGAGTCCTTCCACGATACC; ACOT11 Forward: GAAGACCCGTGTGGAGAGTG, Reverse: AAGGCATTGTTCACGATGGCT; ALAD Forward: GCTACTTCCACCCACTACTTCG, Reverse: TCAGGAACATCCGTGACAAAG; ACADL Forward: AGGGGATCTGTACTCCGCAG, Reverse: CTCTGTCATTGCTATTGCACCA; ELOVL3 Forward: CTGTTCCAGCCCTATAACTTCG, Reverse: GAATGAGGTTGCCCAATACTCC; ELOVL6 Forward: AACGAGCAAAGTTTGAACTGAGG, Reverse: TCGAAGAGCACCGAATATACTGA; ENO3 Forward: GGCTGGTTACCCAGACAAGG, Reverse: TCGTACTTCCCATTGCGATAGAA.

Statistical analysis

Data analysis was conducted in R (version 4.0.3). Quantitative data were presented as the mean ± standard deviation (SD). Differences in means between two groups were assessed using independent samples t-tests, while differences among three or more groups were analyzed by one-way ANOVA. For significant ANOVA results, post-hoc comparisons (Tukey's test) were conducted to examine pairwise group differences. Prognostic genes were identified through univariate and multivariate Cox regression analysis. Kaplan-Meier survival curves and the log-rank test were used to assess survival differences between stratified groups. In all analyses, statistical significance was defined as $P < 0.05$. The specific significance symbols used in figures are defined as follows: *P < 0.05, **P < 0.01, ***P < 0.001, ns = not significant ($P \geq 0.05$).

Results

Characteristics of CC patients from the TCGA database

To elucidate the prognostic significance of fatty acid metabolism-related genes in colon cancer (CC), this study analyzed their expression in relation to patient survival. Transcriptomic and clinical data were obtained from The Cancer Genome Atlas (TCGA) database. Clinical variables, including age, gender, tumor grade, AJCC stage, TNM classification (T, N, M), survival status, and follow-up time, were subsequently extracted. The final cohort comprised 449 primary CC tumors and 41 adjacent normal tissue samples. Detailed cohort characteristics are presented in **Table 5**.

Identification of fatty acid metabolism-related genes in patients with CC

This study identified fatty acid metabolism-related genes for CC patients according to previous studies [15]. A non-redundant set of 309 fatty acid metabolism-related genes was generated by intersecting three independent sources and removing overlaps (**Figure 1A**). This gene set was then screened for differential expression, identifying 158 genes that were significantly dysregulated between the two sample groups.

To assess the prognostic effect of fatty acid metabolism-related genes, univariate and multivariate Cox proportional hazards regression analyses were performed on the TCGA colon cancer (CC) cohort. By this approach, six genes were independently associated with overall survival ($P < 0.05$) (**Figure 1B**). The detailed prognostic information (hazard ratios and confidence intervals) for these six genes is presented in the forest plot (**Figure 1C**).

A prognostic model established with fatty acid metabolism-related genes in CC

These 6 genes were further evaluated by LASSO analysis to decide the number of variables in the prognostic model. Six genes were fitted in the prognostic model based on the minimum cross-validation error in the cross-validation method (**Figure 2A** and **2B**).

Then, all CC patients were assigned a risk score based on the following formula: risk score = (0.705 × expression of ENO3) + (0.528 × expression of ELOVL3) + (-0.416 × expression of ACOT11) + (0.410 × expression of ALAD) + (-0.264 × expression of ELOVL6) + (0.720 × expression of ACADL). We divided all CC patients

Table 3. Composition and volume of reagents for RT-qPCR reaction system

Components of a qPCR	Volume
DNA template	1 μL
Forward primer (10 μM)	0.5 μL
Reverse primer (10 μM)	0.5 μL
2×RealStar Fast SYBR qPCR Mix	10 μL
Sterile Water	Supplement to 20 μL

Table 4. RT-qPCR amplification reaction conditions and instrument operation parameters

Instrument setup procedure	Temperature	Time	Cycles
Pre-denaturation	95°C	2 min	1
Denaturation	95°C	15 s	40
Annealing	60°C	25 s	40
Extension	72°C	30 s	40

Table 5. Clinicopathologic characteristics of CC patients from TCGA database

Characteristic	Number (%)
Age (years)	
≤ 65	190 (41.39)
> 65	269 (58.61)
Gender	
Male	243 (52.94)
Female	216 (47.06)
T stage	
T1-2	89 (19.39)
T3-4	369 (80.39)
Unknow	1 (0.22)
N stage	
N0	270 (58.82)
N1-3	189 (41.18)
M stage	
M0	337 (73.42)
M1	65 (14.16)
Unknow	57 (12.42)
UICC stage	
Stage I-II	254 (55.34)
Stage III-IV	194 (42.26)
Unknow	11 (2.40)
Survival status	
Alive	357 (77.78)
Dead	102 (22.22)

into high- and low-risk groups according to the median risk score. Principal component analysis (PCA) analysis showed that the genes involved in model construction could distinguish between patients at high and low risk, and the results were significantly better than those of fatty acid metabolism-related genes (**Figure 2C** and **2D**). Moreover, the proportion of deceased patients rose significantly with increasing risk scores, with a markedly higher mortality rate observed in the high-risk score interval (**Figure 2E**).

Validation of the fatty acid metabolism-related prognostic model in CC

To further validate the prognostic model, we evaluated the difference in survival between the high and low-risk groups. K-M survival analysis showed that OS in the high-risk group was significantly worse than that in the low-risk group ($P < 0.001$), and PFS was also worse than that in the low-risk group ($P < 0.001$) (**Figure 3A** and **3B**). Meanwhile, the AUCs of 1-year, 2-years, and 3-years were 0.673, 0.727, and 0.746, respectively (**Figure 3C**). The prognostic model AUC was significantly higher than that of clinical characteristics, including age, gender, and stage (**Figure 3D**).

Then we performed the univariate and multivariate Cox regression analyses. We found that age ($P = 0.008$), stage ($P < 0.001$), T status ($P < 0.001$), N status ($P < 0.001$), M status ($P < 0.001$) and risk score ($P < 0.001$) were related to overall survival of CC in the univariate Cox regression analysis (**Figure 3E**). The multivariate Cox regression analysis showed that the prognostic model was an independent prognostic indicator (**Figure 3F**).

Nomogram system for CC patients and DCA

We developed a prognostic nomogram by combining the risk score with clinical factors (age, gender, TNM status, AJCC stage) to predict 1-, 3-, and 5-year survival in CC (**Figure 4A**). Each factor contributes a specific point value; a higher total score correlates with a worse prognosis. The model's performance was validated through calibration plots showing close align-

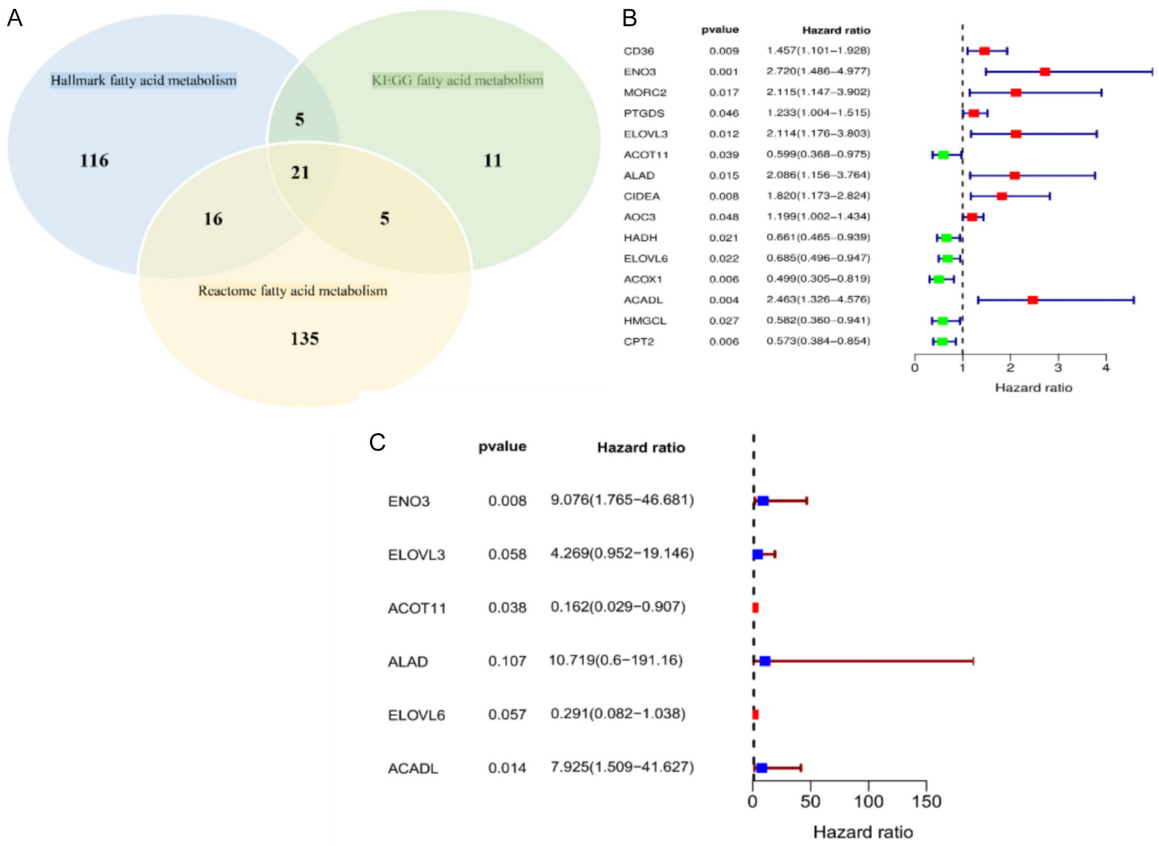

Figure 1. Identified fatty acid metabolism-related genes correlated with prognosis. A. Three fatty acid metabolism-related gene sets. B, C. Univariate and multivariate Cox regression analysis fatty acid metabolism-related genes correlated with prognosis.

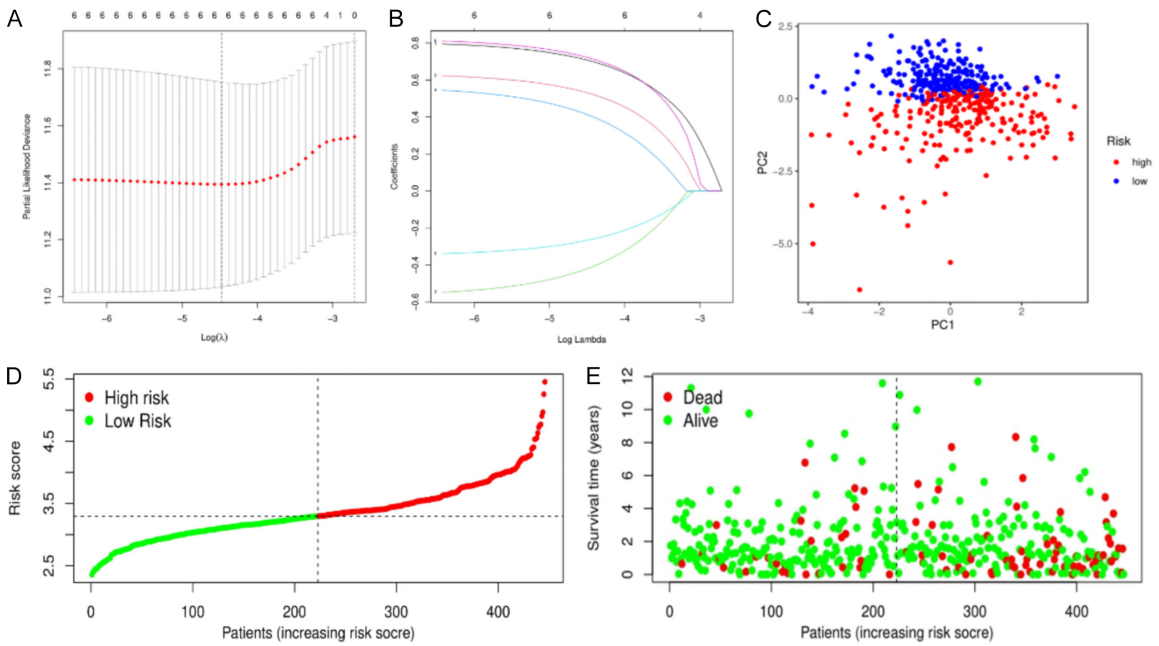

Figure 2. Prognostic model established with fatty acid metabolism-related genes in CC. A, B. LASSO analysis of prognostic fatty acid metabolism-related genes. C. PCA shows the power prediction ability of the prognostic model. D, E. The distribution of risk score and survival status of each patient.

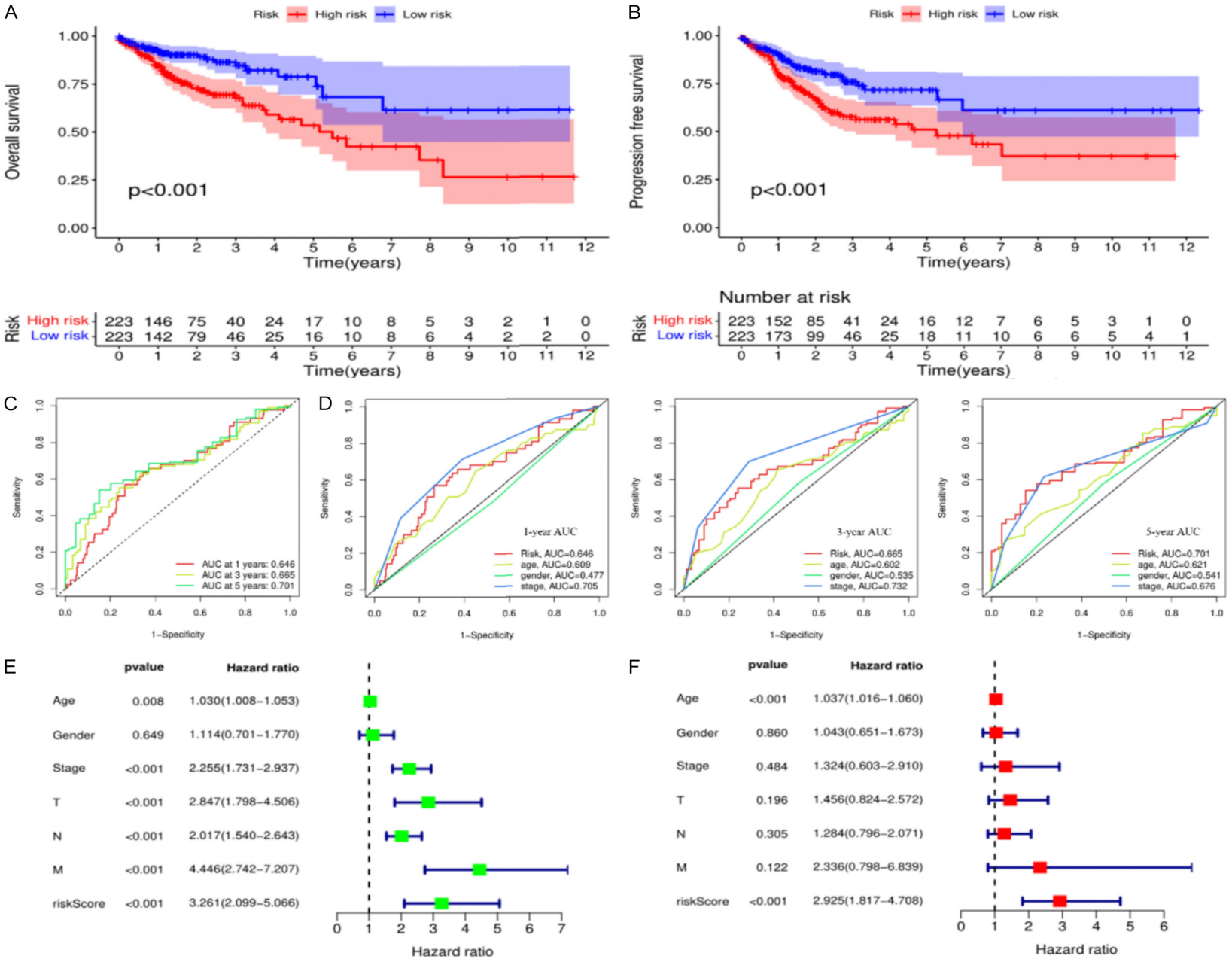
A
Risk High risk Low risk
Overall survival
p<0.001
Time(years)
Risk High risk 223 146 75 40 24 17 10 8 5 3 2 1 0
Low risk 223 142 79 46 25 16 10 8 6 4 2 2 0
B
Risk High risk Low risk
Progression free survival
p<0.001
Time(years)
Number at risk
Risk High risk 223 152 85 41 24 16 12 7 6 5 3 1 0
Low risk 223 173 99 46 25 18 11 10 6 6 5 4 1
C
Sensitivity
1−Specificity
AUC at 1 years: 0.646
AUC at 3 years: 0.665
AUC at 5 years: 0.701
D
1-year AUC
Risk, AUC=0.646
age, AUC=0.609
gender, AUC=0.477
stage, AUC=0.705
3-year AUC
Risk, AUC=0.665
age, AUC=0.602
gender, AUC=0.535
stage, AUC=0.732
5-year AUC
Risk, AUC=0.701
age, AUC=0.621
gender, AUC=0.541
stage, AUC=0.676
E
pvalue Hazard ratio
Age 0.008 1.030(1.008−1.053)
Gender 0.649 1.114(0.701−1.770)
Stage <0.001 2.255(1.731−2.937)
T <0.001 2.847(1.798−4.506)
N <0.001 2.017(1.540−2.643)
M <0.001 4.446(2.742−7.207)
riskScore <0.001 3.261(2.099−5.066)
Hazard ratio
F
pvalue Hazard ratio
Age <0.001 1.037(1.016−1.060)
Gender 0.860 1.043(0.651−1.673)
Stage 0.484 1.324(0.603−2.910)
T 0.196 1.456(0.824−2.572)
N 0.305 1.284(0.796−2.071)
M 0.122 2.336(0.798−6.839)
riskScore <0.001 2.925(1.817−4.708)
Hazard ratio

Figure 3. Evaluation of predictive value of prognostic models. A, B. Kaplan-Meier curves for patients in the high- and low-risk groups. C. ROC curves analysis of prognostic model at 1 year, 2 years, and 3 years. D. ROC curves analysis of other clinical characteristics at 1 year, 2 years, and 3 years. E, F. Univariate Cox regression analysis and multivariate Cox regression analysis (*ns = not significant (P ≥ 0.05),*P < 0.05, **P < 0.01, ***P < 0.001).

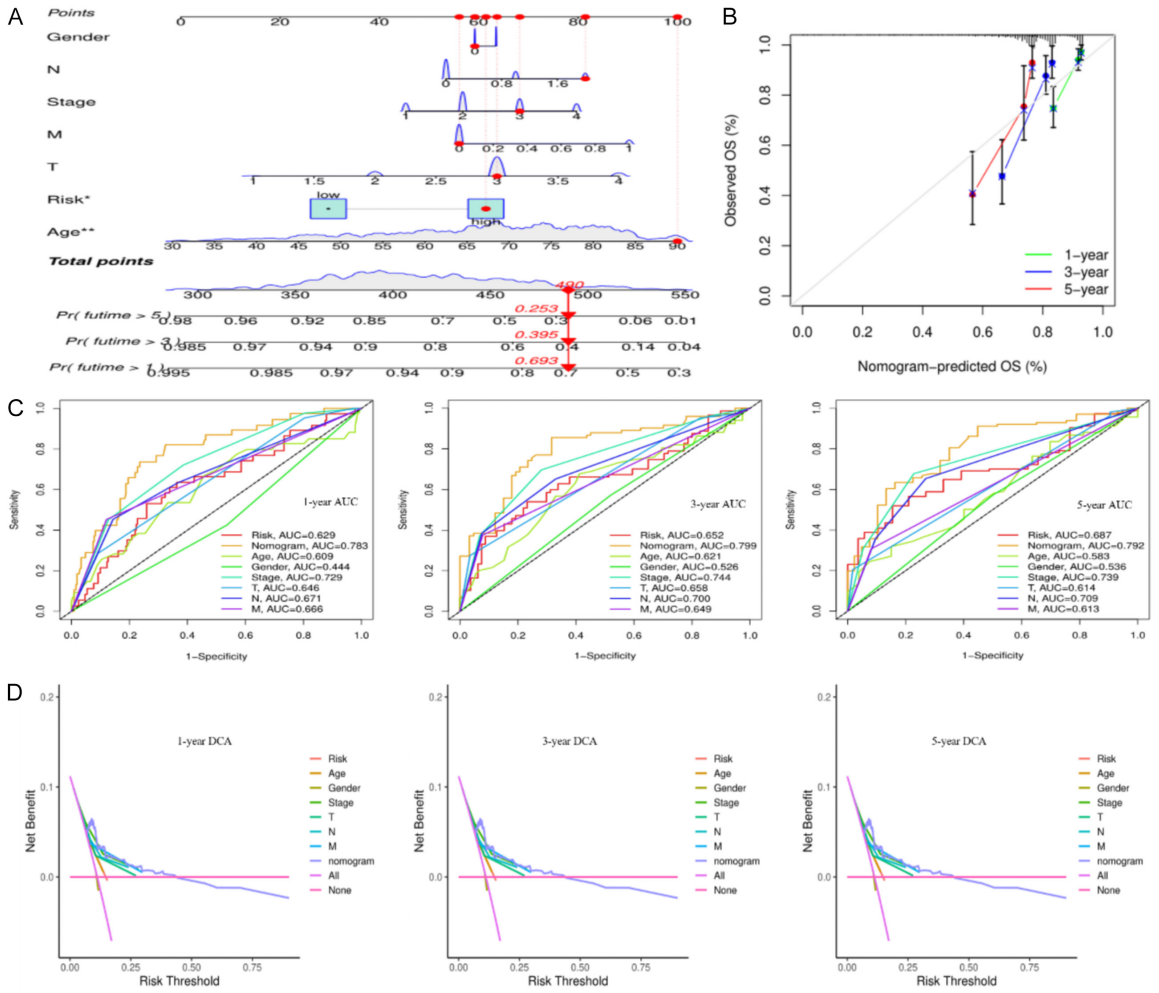

Figure 4. Nomogram system for CC patients. A. Nomogram predicted 1-, 3- and 5-year overall survival using seven prognostic factors. B. The calibration of the nomogram predicted system. C. ROC curves analysis of nomogram system at 1 year, 2 years, and 3 years. D. DCA analysis of nomogram system at 1 year, 2 years, and 3 years.

ment between predicted and actual survival (**Figure 4B**), time-dependent ROC curves with AUCs of 0.783 (1-year), 0.799 (3-year), and 0.792 (5-year) (**Figure 4C**), and decision curve analysis (DCA) demonstrating superior net clinical benefit over standard clinical parameters within a 0-45% risk threshold (**Figure 4D**).

Molecular characteristics of high- and low-risk groups

Biologic pathway differences between risk groups were assessed using Gene Set Variation Analysis (GSVA). The high-risk group showed significant enrichment in multiple KEGG pathways, notably those involved in biosynthesis (e.g., glycosaminoglycan, glycans, fatty acids) and key oncogenic signaling (Notch and p53) (**Figure 5A**). Gene Ontology (GO) analysis further highlighted enrichment in specific metabolic processes, including fatty acid metabolism and GTP metabolism (**Figure 5B**).

Immune cell infiltration and immune checkpoint in high- and low-risk groups

To further investigate the association between the risk score and tumor immune microenviron-

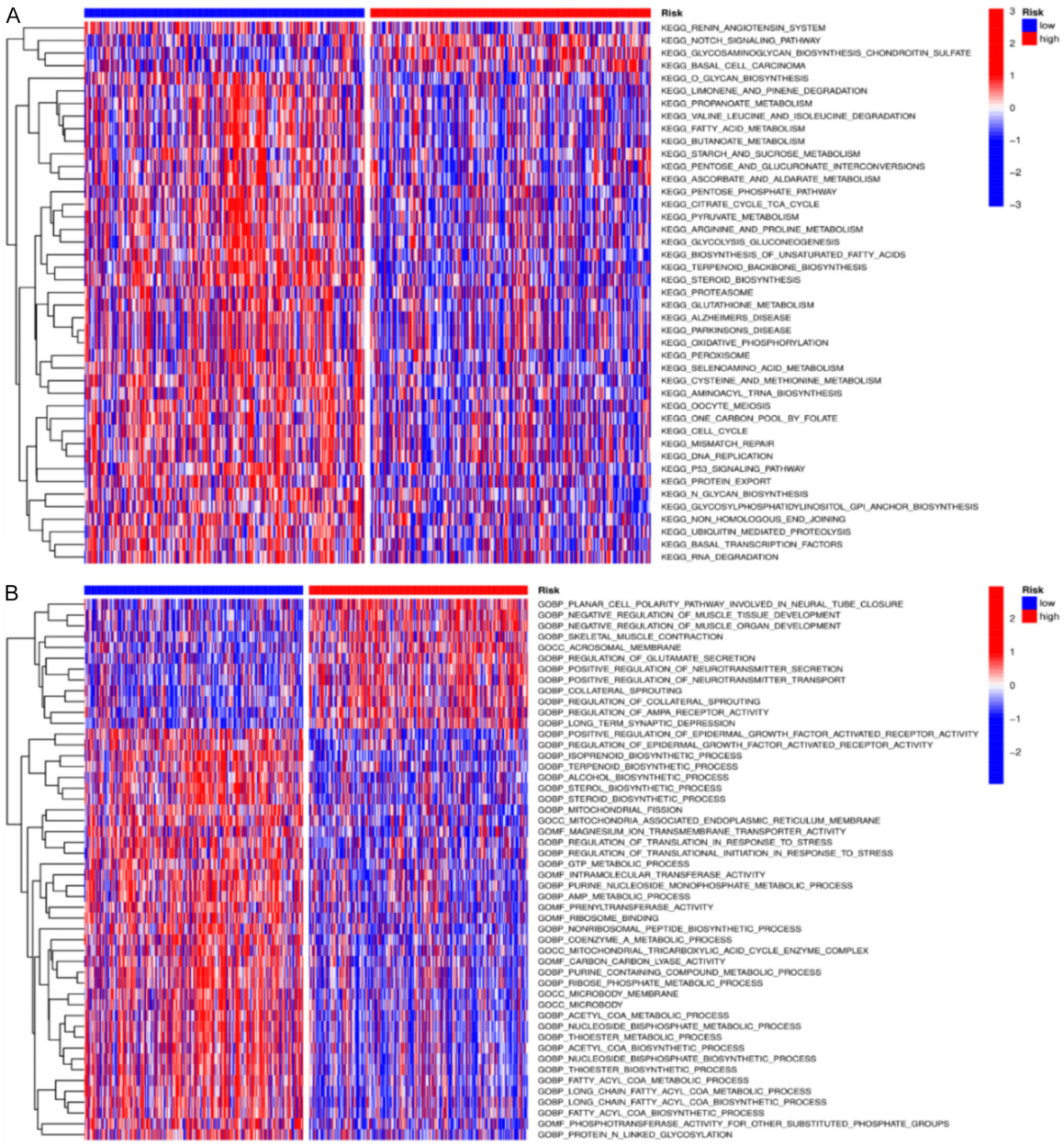

Figure 5. GSEA functional enrichment analysis. A, B. GEVA analyzes KEGG and GO databases.

ment, we quantified the relative abundance of immune cell subsets and activity of immune-related pathways using single-sample Gene Set Enrichment Analysis (ssGSEA). Significant differences were observed between high- and low-risk groups as determined by independent sample t-tests in the infiltration levels of macrophages, natural killer (NK) cells, T helper cells, T helper 2 (Th2) cells, and regulatory T cells (Tregs), suggesting a more active or dysregulated immune state in high-risk patients (**Figure 6A**). Analysis of immune checkpoint expression revealed significantly higher levels of LAG3, PDCD1, and CTLA4 in the high-risk group, whereas CD274 (PD-L1) expression showed no significant intergroup difference (**Figure 6C**). Furthermore, assessment of immunotherapy response potential by the Tumor Immune Dysfunction and Exclusion (TIDE) algorithm indicated that the high-risk group exhibited higher TIDE scores, implying a greater likelihood of immune escape and a poorer predicted res-

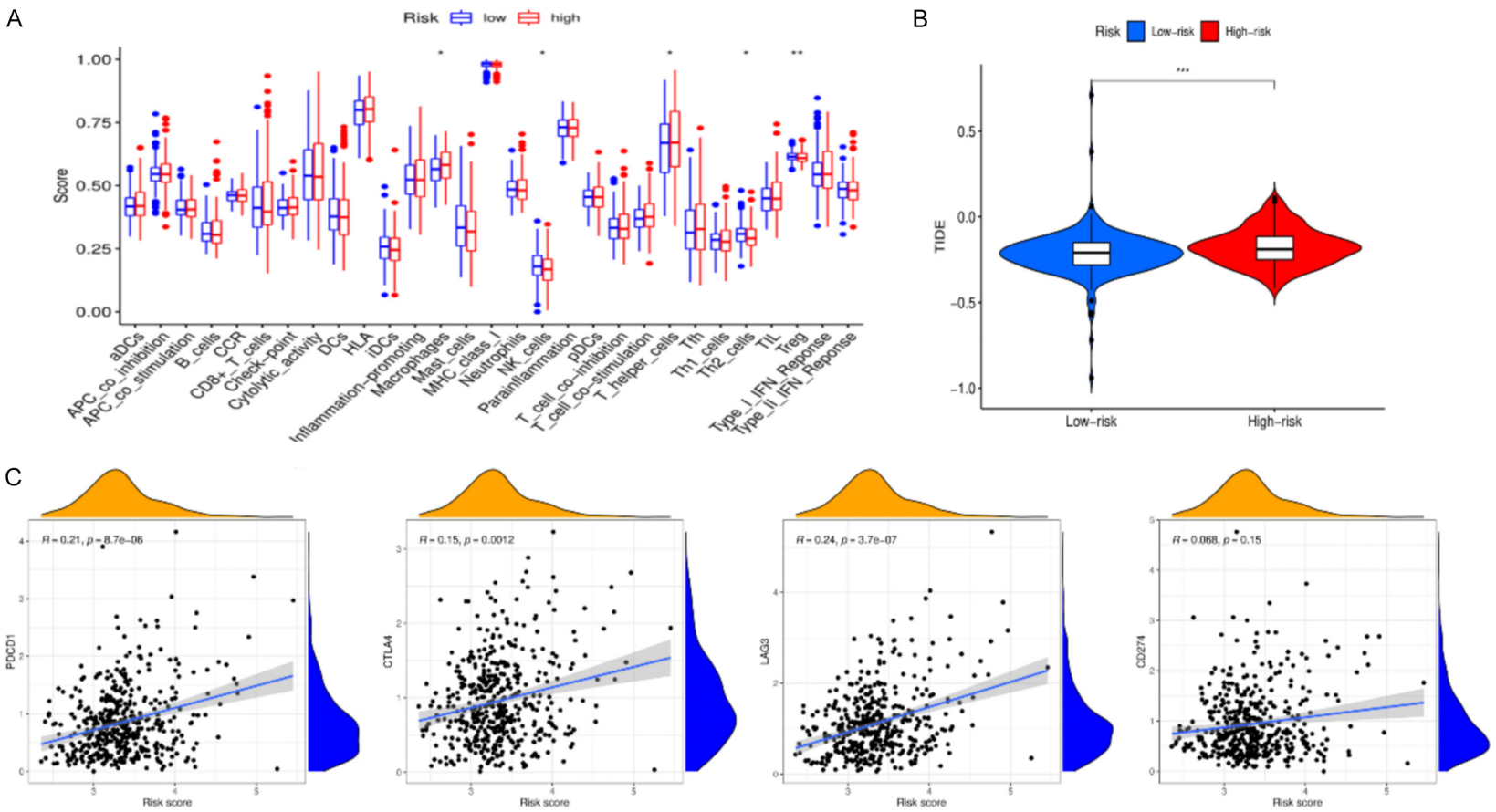

Figure 6. Immune function analysis. A. The boxplots display the scores of 16 immune cells and 13 immune-related functions. B. The TIDE score of high- and low-risk groups. C. Correlation between some important immune checkpoints and the risk score.

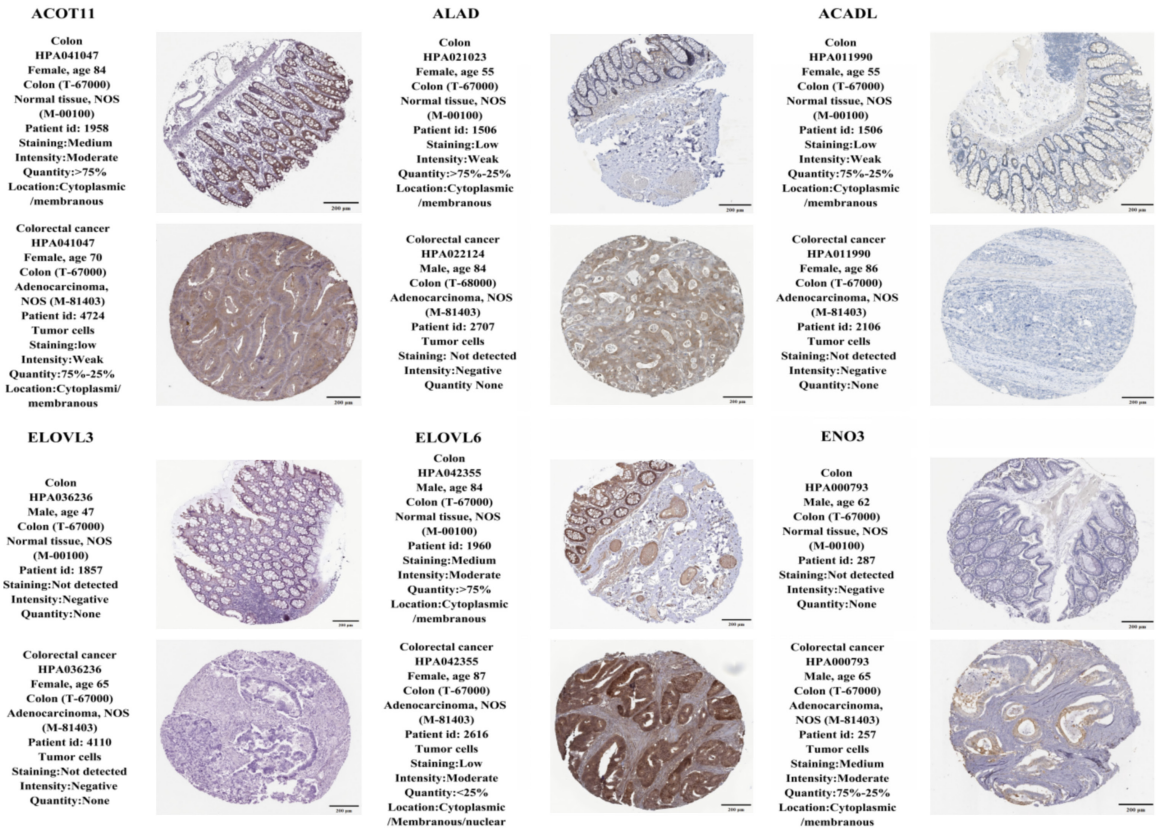

Figure 7. IHC staining showed the expression levels of 6 fatty acid metabolism-related genes (Scale: 1 cm = 10 units).

ponse to immunotherapy (**Figure 6B**). Collectively, these findings suggest that the risk score could serve as a valuable biomarker to stratify patients for immunotherapeutic strategies in colon cancer.

Validation of the expression levels of 6 fatty acid metabolism-related risk genes in CC and normal colon tissues

We validated the protein expression of selected fatty acid metabolism genes by analyzing publicly available immunohistochemistry images from the Human Protein Atlas (HPA). The results indicated lower expression of ACOT11, ALAD, ELOVL6, and ACADL, but higher expression of ENO3, in CC tissues relative to normal controls based on independent samples t-tests. ELOVL3 expression showed no significant tumor-normal difference (**Figure 7**).

mRNA expression levels of the risk genes

We analyzed the differential expression of the six identified fatty acid metabolism (FAM)-related genes between colon cancer (CC) tumors and adjacent normal tissues within the TCGA cohort by independent samples t-tests. As illustrated in **Figure 8A-F**, the mRNA expression levels of ACOT11, ALAD, ACADL, and ELOVL6 were significantly downregulated in tumor tissues compared to normal controls ($P < 0.01$). Conversely, ELOVL3 and ENO3 expression was significantly upregulated in CC samples (**Figure 8A-F**, $P < 0.01$).

Validation of the expression of the risk genes in colon cancer cell lines

Real time quantitative PCR (qRT-PCR) was utilized to compare the difference in mRNA expression of (A) ACOT11, (B) ALAD, (C) ACADL, (D) ELOVL3, (E) ELOVL6, (F) ENO3 among the NCM-460 normal colon epithelial cell line and the SW480 and HCT116 colon cancer cell lines. Differences were analyzed using one-way ANOVA, and significant overall differences were followed by Tukey's post-hoc test for pairwise comparisons. Consistent with the bioinformatic analysis, ENO3 and ELOVL6 expression was

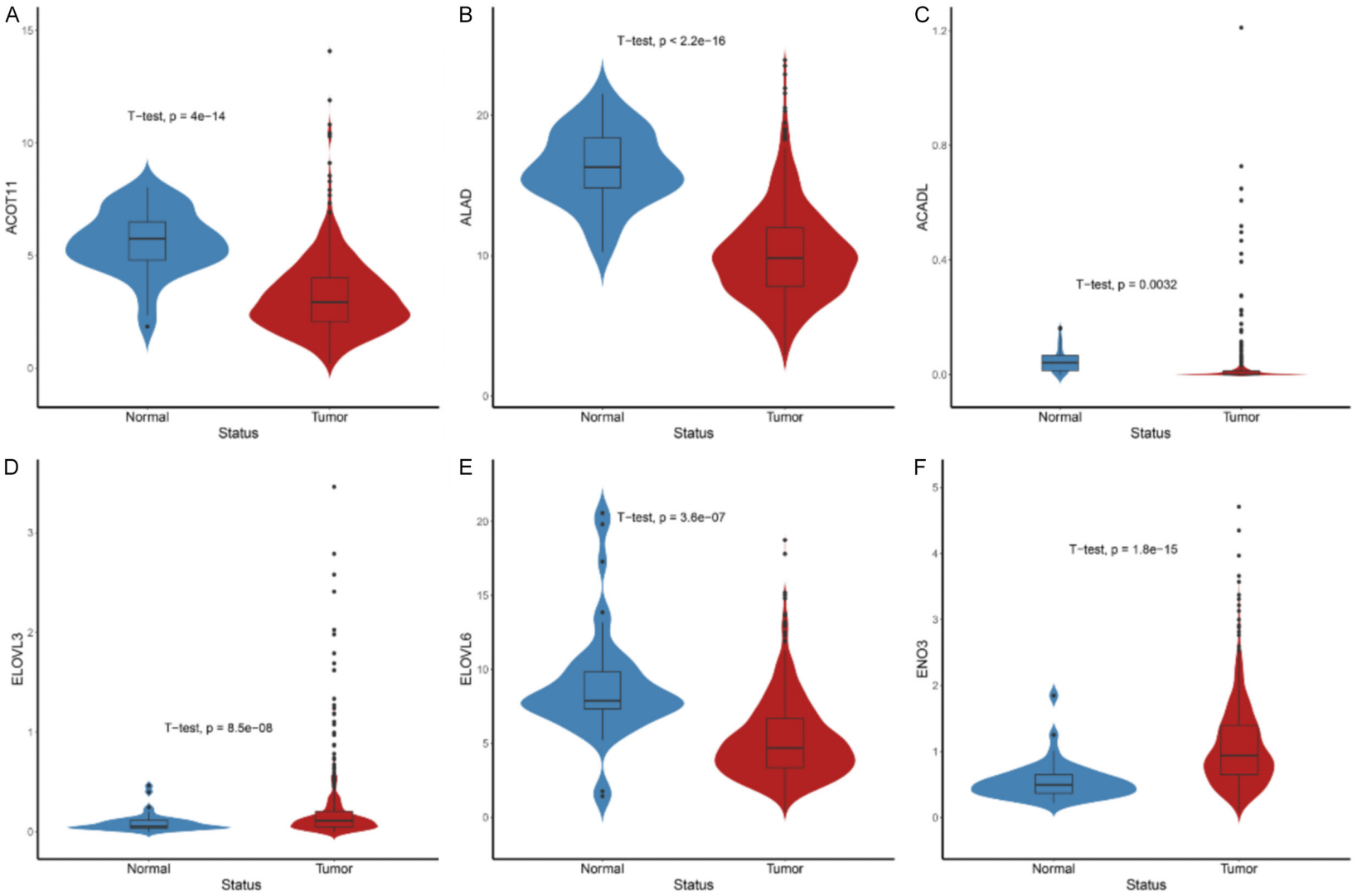

Figure 8. Differential expression of 6 fatty acid metabolism-related genes in TCGA. Difference in mRNA expression of (A) ACOT11, (B) ALAD, (C) ACADL, (D) ELOVL3, (E) ELOVL6, (F) ENO3 between normal and colon cancer tissues (ns = not significant (P ≥ 0.05), *P < 0.05, **P < 0.01, ***P < 0.001).

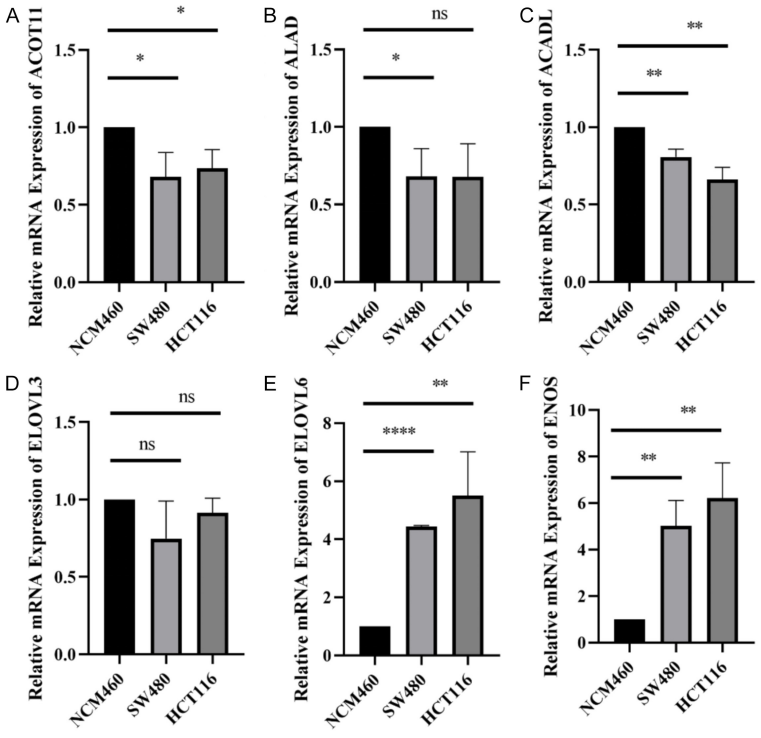

Figure 9. Relative mRNA expression of 6 fatty acid metabolism-related genes. Real time quantitative PCR was utilized to compare the difference in mRNA expression of (A) ACOT11, (B) ALAD, (C) ACADL, (D) ELOVL3, (E) ELOVL6, (F) ENO3 among the NCM460 normal colon epithelial cell line and the SW480 and HCT116 colon cancer cell lines (ns: No significance($P \geq 0.05$), *$P < 0.05$, **$P < 0.01$, ****$P < 0.0001$).

significantly upregulated in cancer cell lines (**Figure 9E**, **9F**; $P < 0.05$). In contrast, ACOT11, ALAD, and ACADL were significantly downregulated (**Figure 9A-C**; $P < 0.05$). No significant difference was observed in ELOVL3 expression between the two groups (**Figure 9D**; $P>0.05$).

Discussion

A common feature of tumor cells is metabolic reprogramming to meet the energy requirements for rapid tumor cell proliferation [16]. Lipids not only constitute the basic structure of biological membranes but also function as signaling molecules and energy sources. Fatty acids are an important component of lipids, and studies have shown that, owing to its growth in an environment abundant with adipose tissue, colon cancer exhibits a pronounced “lipid addiction”. This means that colon cancer cells tend to invade and spread into the adipose tissue. These cancer cells can uptake fatty acids from the surrounding adipose tissue and undergo fatty acid oxidation, which provides energy for the growth of colon cancer cells and subsequently promotes the invasion and metastasis of tumor cells [6, 17]. CC is a malignant tumor with high morbidity and mortality. Exploring the role of different fatty acid metabolism genes in CC is important for discovering new strategies for tumor therapy.

In this study, we summarized fatty acid metabolism genes through three gene sets. Univariate and multivariate Cox proportional risk regression analyses were performed to screen out six fatty acid metabolism genes (ENO3, ELOVL3, ACOT11, ALAD, ELOVL6, ACADL) closely related to prognosis. The key genes related to fatty acid metabolism were further screened by LASSO regression and cross-validation, and the prognostic model was constructed. These six fatty acid metabolism genes were abnormally expressed in multiple tumor tissues and were closely related to tumor progression. However, the role of these genes in the prognosis of CC remains to be studied. ENO3 is an enzyme that catalyzes the formation of phosphoenolpyruvate from 2-phosphoglycerate. ENO3 can promote the proliferation and migration of colorectal cancer by enhancing cell glycolysis [18]. ELOVL3 and ELOVL6 are rate-limiting enzymes that catalyze the synthesis of very long-chain fatty acids. Dysfunctional ELOVL3 has been reported to be associated with various diseases, including cancers. In prostate cancer, ELOVL3 transcriptional upregulation is closely associated with prostate cancer invasion and migration [19]. ELOVL6 is associated with poor prognosis in HCC patients by promoting cell proliferation and Akt activation [20]. ACOT11 can encode enzymatic hydrolysis of fatty acid acyl CoA esters into free fatty acids and CoA. A high expression of ACOT11 in lung cancer patients is positively correlated with poor prognosis. ACOT11 is involved in tumor invasion and migration, and promotes cell apoptosis [21]. Overexpression of ALAD in breast cancer patients can inhibit epithelial-mesenchymal transition [22]. ACADL, a key enzyme in the first

step of mitochondrial fatty acid β-oxidation, is expressed at reduced levels in hepatocellular carcinoma (HCC) and exerts tumor-suppressive effects through Hippo/YAP signaling [23]. ACADL inhibits HCC metastasis by suppressing the expression of MMP14 through the STAT3 signaling pathway [24]. However, the relevant role of this gene in fatty acid oxidation in CC is unclear. In this study, ACADL expression was down-regulated and correlated with the prognosis of CC patients. It was incorporated into the construction of the prognostic model for HCC patients, further demonstrating the important role of this gene for the development and progression of colon cancer.

We developed a six-gene prognostic signature that stratified patients by median risk score. The model demonstrated good predictive accuracy, as evidenced by PCA, ROC, and risk curve analyses. Crucially, multivariate analysis established the risk score as an independent prognostic factor after adjustment for age and pathologic stage (TNM), confirming its standalone value in predicting CC outcome.

Next, we further analyzed the function of immune cells in the high and low-risk populations, and the results showed that the immune cells in the high-risk group were more activated, and the related functions of immune cells were more active. Specifically, the expression level of macrophages and T helper cells was higher, and the expression level of Tregs was lower in the high-risk population. This may be related to the overactivation of the immune system in patients with early colon cancer. Previous studies have shown that increased M2 polarization in macrophages promotes colon cancer growth [25-27]. Salman found that in the CC microenvironment, the infiltration of highly immunosuppressed Treg cells was significantly increased, and these increased Tregs may hinder the response of CRC patients to immune checkpoint blockade. However, the effects of different immune checkpoint inhibitory mechanisms on Treg level or activity need to be further studied [28]. Thus, targeting these immune cells offers the possibility of immunotherapy for colon cancer.

PD-1 (PDCD-1), PD-L1 (CD274), LAG3, and CTLA4 are important immune checkpoints. Abnormal activation of immune checkpoints on tumor cells contributes to the immune escape of tumor cells. Immune checkpoint inhibitors have been applied increasingly applied in various malignant tumors, proving their therapeutic potential. In melanoma patients [29], ipilimumab (CTLA4 inhibitor) and nivolumab (PD-1 inhibitor) have a significant survival benefit, and nivolumab plus ipilimumab has a more durable survival benefit. Our results showed that the expression levels of PD-1, LAG3, and CTLA4 were higher in high-risk patients, suggesting that targeted immune checkpoints such as PD-1, LAG3, and CTLA4 may improve the efficacy of immunotherapy in CC patients. Finally, TIDE scores of the high and low-risk groups were calculated respectively [30], and the results showed that the probability of immune escape was higher in the high-risk group, and the therapeutic effect of immune checkpoint blockade was worse.

Then, we incorporated the prognostic score into the prediction model, and a nomogram was constructed. The nomogram prediction model's accuracy was evaluated using calibration plots, ROC curve, and DCA. DCA is a new method to evaluate clinical predictive models [31]. The above three methods demonstrate the practicality of the prognostic model, which can help us timely identify patients with poor prognoses and specify individualized treatment plans to further improve the survival rate of CC patients.

The following limitations of our research should be taken into consideration. First, our study analyzed only the prognostic role of fatty acid metabolism-related genes using colon cancer data from the TCGA database, without collecting clinical data for further validation to confirm a greater value of our research. Second, in our study, we did not explain how these fatty acid metabolism-related genes affect tumor growth, leading to differences in patient prognosis. Future research should delve deeper into how lipids promote tumor cell growth. Finally, despite these limitations, our study, as a novel research approach, still suggests that alterations in fatty acid metabolism-related genes may be a reliable therapeutic target for cancer patients.

In summary, we developed and validated a robust prognostic signature based on six fatty acid metabolism-related genes for colon cancer (CC). Furthermore, we constructed a clini-

cally applicable nomogram by integrating this signature with key clinicopathologic factors. Our findings not only highlight the prognostic value of fatty acid metabolism but also position these genes as promising therapeutic targets, paving the way for personalized treatment strategies to improve survival.

Disclosure of conflict of interest

None.

Address correspondence to: Xuan Wang, Department of Pathology, First Affiliated Hospital of Xi'an Jiaotong University, Xi'an 710061, Shaanxi, China. Tel: +86-18392885407; E-mail: wangxuan19950422@163.com

References

[1] Li Q, Xia C, Li H, Yan X, Yang F, Cao M, Zhang S, Teng Y, He S, Cao M and Chen W. Disparities in 36 cancers across 185 countries: secondary analysis of global cancer statistics. Front Med 2024; 18: 911-920.

[2] Siegel RL, Kratzer TB, Giaquinto AN, Sung H and Jemal A. Cancer statistics, 2025. CA Cancer J Clin 2025; 75: 10-45.

[3] Kumar R, Harilal S, Carradori S and Mathew B. A Comprehensive overview of colon cancer- a grim reaper of the 21st century. Curr Med Chem 2021; 28: 2657-2696.

[4] Xia L, Oyang L, Lin J, Tan S, Han Y, Wu N, Yi P, Tang L, Pan Q, Rao S, Liang J, Tang Y, Su M, Luo X, Yang Y, Shi Y, Wang H, Zhou Y and Liao Q. The cancer metabolic reprogramming and immune response. Mol Cancer 2021; 20: 28.

[5] Huang X, Sun Y, Song J, Huang Y, Shi H, Qian A, Cao Y, Zhou Y and Wang Q. Prognostic value of fatty acid metabolism-related genes in colorectal cancer and their potential implications for immunotherapy. Front Immunol 2023; 14: 1301452.

[6] Winkelkotte AM, Al-Shami K, Chaves-Filho AB, Vogel FCE and Schulze A. Interactions of fatty acid and cholesterol metabolism with cellular stress response pathways in cancer. Cold Spring Harb Perspect Med 2025; 15: a041548.

[7] Masetti M, Carriero R, Portale F, Marelli G, Morina N, Pandini M, Iovino M, Partini B, Erreni M, Ponzetta A, Magrini E, Colombo P, Elefante G, Colombo FS, den Haan JMM, Peano C, Cibella J, Termanini A, Kunderfranco P, Brummelman J, Chung MWH, Lazzeri M, Hurle R, Casale P, Lugli E, DePinho RA, Mukhopadhyay S, Gordon S and Di Mitri D. Lipid-loaded tumor-associated macrophages sustain tumor growth and invasiveness in prostate cancer. J Exp Med 2022; 219: e20210564.

[8] Luo M, Yan J, Hu X, Li H, Li H, Liu Q, Chen Y and Zou Z. Targeting lipid metabolism for ferroptotic cancer therapy. Apoptosis 2023; 28: 81-107.

[9] Nuzzo PV, Rodrigues S, Ribeiro CF, Teixeira IF, Fanelli GN, Bleve S, Ravera F, Pakula H, Pederzoli F, Nanus DM and Loda M. Targeting cancer metabolism: therapeutic potential of the fatty acid synthase (FASN) inhibitors. Crit Rev Oncol Hematol 2025; 214: 104910.

[10] Schlaepfer IR and Joshi M. CPT1A-mediated Fat oxidation, mechanisms, and therapeutic potential. Endocrinology 2020; 161: bqz046.

[11] Tan Z, Xiao L, Tang M, Bai F, Li J, Li L, Shi F, Li N, Li Y, Du Q, Lu J, Weng X, Yi W, Zhang H, Fan J, Zhou J, Gao Q, Onuchic JN, Bode AM, Luo X and Cao Y. Targeting CPT1A-mediated fatty acid oxidation sensitizes nasopharyngeal carcinoma to radiation therapy. Theranostics 2018; 8: 2329-2347.

[12] Xiong X, Wen YA, Fairchild R, Zaytseva YY, Weiss HL, Evers BM and Gao T. Upregulation of CPT1A is essential for the tumor-promoting effect of adipocytes in colon cancer. Cell Death Dis 2020; 11: 736.

[13] Wu L, Zhang X, Zheng L, Zhao H, Yan G, Zhang Q, Zhou Y, Lei J, Zhang J, Wang J, Xin R, Jiang L, Peng J, Chen Q, Lam SM, Shui G, Miao H and Li Y. RIPK3 orchestrates fatty acid metabolism in tumor-associated macrophages and hepatocarcinogenesis. Cancer Immunol Res 2020; 8: 710-721.

[14] Jiang N, Xie B, Xiao W, Fan M, Xu S, Duan Y, Hamsafar Y, Evans AC, Huang J, Zhou W, Lin X, Ye N, Wanggou S, Chen W, Jing D, Fragoso RC, Dugger BN, Wilson PF, Coleman MA, Xia S, Li X, Sun LQ, Monjazeb AM, Wang A, Murphy WJ, Kung HJ, Lam KS, Chen HW and Li JJ. Fatty acid oxidation fuels glioblastoma radioresistance with CD47-mediated immune evasion. Nat Commun 2022; 13: 1511.

[15] Zhao SS, Bai RR, Zhang BH, Sun XR, Huang N, Chen Y, Sun ZJ, Sun LM, Zhang Y and Cui ZQ. Investigating the diagnostic and prognostic significance of genes related to fatty acid metabolism in hepatocellular carcinoma. BMC Gastroenterol 2024; 24: 409.

[16] Liao M, Yao D, Wu L, Luo C, Wang Z, Zhang J and Liu B. Targeting the Warburg effect: a revisited perspective from molecular mechanisms to traditional and innovative therapeutic strategies in cancer. Acta Pharm Sin B 2024; 14: 953-1008.

[17] Jin Z, Chai YD and Hu S. Fatty acid metabolism and cancer. Adv Exp Med Biol 2021; 1280: 231-241.

[18] Chen J, Zhang Z, Ni J, Sun J, Ju F, Wang Z, Wang L and Xue M. ENO3 promotes colorectal cancer progression by enhancing cell glycolysis. Med Oncol 2022; 39: 80.

[19] Yang Y, Liu L, Li M, Cheng X, Fang M, Zeng Q and Xu Y. The chromatin remodeling protein

BRG1 links ELOVL3 trans-activation to prostate cancer metastasis. Biochim Biophys Acta Gene Regul Mech 2019; 1862: 834-845.
[20] Su YC, Feng YH, Wu HT, Huang YS, Tung CL, Wu P, Chang CJ, Shiau AL and Wu CL. Elovl6 is a negative clinical predictor for liver cancer and knockdown of Elovl6 reduces murine liver cancer progression. Sci Rep 2018; 8: 6586.
[21] Liang C, Wang X, Zhang Z, Xiao F, Feng H, Ma Q, Huang J, Qiang G, Zhong D and Liu D. ACOT11 promotes cell proliferation, migration and invasion in lung adenocarcinoma. Transl Lung Cancer Res 2020; 9: 1885-1903.
[22] Ge J, Yu Y, Xin F, Yang ZJ, Zhao HM, Wang X, Tong ZS and Cao XC. Downregulation of delta-aminolevulinate dehydratase is associated with poor prognosis in patients with breast cancer. Cancer Sci 2017; 108: 604-611.
[23] Li L, Wang LL, Wang TL and Zheng FM. ACADL suppresses PD-L1 expression to prevent cancer immune evasion by targeting Hippo/YAP signaling in lung adenocarcinoma. Med Oncol 2023; 40: 118.
[24] Guo D, Zhang X, Cui H, Yu D, Zhang H, Shi X, Pang C, Li J, Guo W and Zhang S. ACADL functions as a tumor suppressor in hepatocellular carcinoma metastasis by inhibiting matrix metalloproteinase 14. Front Oncol 2022; 12: 821484.
[25] Zhang M, Li X, Zhang Q, Yang J and Liu G. Roles of macrophages on ulcerative colitis and colitis-associated colorectal cancer. Front Immunol 2023; 14: 1103617.
[26] Wang L, Li S, Luo H, Lu Q and Yu S. PCSK9 promotes the progression and metastasis of colon cancer cells through regulation of EMT and PI3K/AKT signaling in tumor cells and phenotypic polarization of macrophages. J Exp Clin Cancer Res 2022; 41: 303.
[27] Jiang X, Cao G, Gao G, Wang W, Zhao J and Gao C. Triptolide decreases tumor-associated macrophages infiltration and M2 polarization to remodel colon cancer immune microenvironment via inhibiting tumor-derived CXCL12. J Cell Physiol 2021; 236: 193-204.
[28] Toor SM, Murshed K, Al-Dhaheri M, Khawar M, Abu Nada M and Elkord E. Immune checkpoints in circulating and tumor-infiltrating CD4+ T cell subsets in colorectal cancer patients. Front Immunol 2019; 10: 2936.
[29] Liang L, Kuang X, He Y, Zhu L, Lau P, Li X, Luo D, Gong L, Zhou W, Zhang F, Liang X, Li Z, Hu B, Liu D, Ding T, Li H, Zhao S, Su J, Hung MC, Liu J, Liu H and Chen X. Alterations in PD-L1 succinylation shape anti-tumor immune responses in melanoma. Nat Genet 2025; 57: 680-693.
[30] Fu J, Li K, Zhang W, Wan C, Zhang J, Jiang P and Liu XS. Large-scale public data reuse to model immunotherapy response and resistance. Genome Med 2020; 12: 21.
[31] Wen X, Sun H, Du S, Xia J, Zhang W and Zhang F. A nomogram of inflammatory indexes for preoperatively predicting the risk of lymph node metastasis in colorectal cancer. Tech Coloproctol 2024; 28: 148.